Published in final edited form as:
Biol Chem. 2010 August ; 391(8): 937–945. doi:10.1515/BC.2010.080.

Deletion of cathepsin H perturbs angiogenic switching, vascularization and growth of tumors in a mouse model of pancreatic islet cell cancer

Vasilena Gocheva[1,2], **Xiaoping Chen**[1], **Christoph Peters**[3], **Thomas Reinheckel**[3], and **Johanna A. Joyce**[1,*]

[1]Cancer Biology and Genetics Program, Memorial Sloan Kettering Cancer Center, New York, NY 10021, USA

[2]Weill-Graduate School of Medical Sciences, Cornell University, New York, NY 10021, USA

[3]Institute for Molecular Medicine and Cell Research, Albert Ludwigs University, Freiburg, Germany

Abstract

Proteases can regulate many aspects of tumor development as their actions, which include degradation of the extracellular matrix, proteolytic processing of chemokines and activation of other enzymes, influence a number of key tumorigenic processes. Members of one protease class, the cysteine cathepsins, have received increasing recognition for their involvement in cancer development, and numerous clinical studies have reported correlations between elevated cathepsin levels and malignant progression. This is also the case for cathepsin H, a member of the cysteine cathepsin family, and its utility as a prognostic marker has been analyzed extensively. However, there is limited information available on its specific functions in tumor development and progression. To gain further insight into the role of this protease in cancer, we crossed *cathepsin H* deficient mice to the RIP1-Tag2 model of pancreatic islet carcinogenesis. Deletion of *cathepsin H* significantly impaired angiogenic switching of the pre-malignant hyperplastic islets and resulted in a reduction in the subsequent number of tumors that formed. Moreover, the tumor burden in *cathepsin H* null RT2 mice was significantly reduced, in association with defects in the blood vasculature and increased apoptosis. Thus, we demonstrate here, for the first time, important tumor promoting roles for cathepsin H *in vivo* using a mouse model of human cancer.

Keywords

Cancer; cathepsin H; mouse model; pancreatic endocrine cancer; protease

Introduction

Critical roles for proteases have been proposed in multiple processes during cancer development and progression that require protein turnover and degradation, including tumor invasion, angiogenesis and metastasis. Different protease families have been implicated in malignant progression, and one such class of enzymes is the cysteine cathepsins, a group of papain-like cysteine proteases with important functions in different physiological processes (Brix et al., 2008; Reinheckel et al., 2008; Vasiljeva et al., 2007).

*Correspondence: joycej@mskcc.org, 1275 York Avenue, Box 372, New York, NY 10021, FAX (646) 422-0231; PHONE (646) 888-2048.

There are eleven cysteine cathepsins in the human genome (cathepsin B, C, F, H, K, L, L2/V, O, S, W, X/Z), and while most of them are endopeptidases, certain family members such as cathepsin B and H can additionally function as exopeptidases, (Lecaille et al., 2002). The aminopepeptidase activity of cathepsin H is determined by a “mini-chain” that limits the access of substrates to the catalytic center (Vasiljeva et al., 2003). The potent proteolytic activity of cathepsins is known to affect the fate of many intracellular as well as extracellular targets, and deregulation of these functions is associated with a number of disease states including cancer. The role of several cathepsins has been studied in cancer development, and their utility as prognostic markers has been evaluated for numerous different tumor types (Berdowska, 2004). Most of the research to date has focused on cathepsins B and L, while other members of the family, such as cathepsin H, have been far less studied and their role in cancer progression remains contradictory.

Several studies have found a correlation between elevated cathepsin H levels and increased malignancy in multiple tumor types, suggesting that this protease may have important tumor-promoting properties. For example, elevated levels of cathepsin H have been found in gliomas (Sivaparvathi et al., 1996), colorectal carcinoma (del Re et al., 2000), prostate cancer (Waghray et al., 2002) and breast cancer (Gabrijelcic et al., 1992), and in all cases this was associated with more aggressive disease. For other cancers, such as melanoma, conflicting reports have been published. Some groups have observed increased cathepsin H expression in metastatic tumors (Kageshita et al., 1995), while others have reported the opposite, finding a reduction in cathepsin H expression and activity in melanocytic lesions compared to normal skin (Fröhlich et al., 2001). Its validity as a universal prognostic factor was further called into question after reports that patients with head and neck cancer not only have lower levels of cathepsin H than the adjacent normal tissue (Kos et al., 1995), but also that high levels of cathepsin H expression correlated with better outcome and increased survival (Budihna et al., 1996). As these studies illustrate, the precise roles of cathepsin H in tumorigenesis are a topic of active debate and further studies are clearly needed to achieve a comprehensive understanding of its biological functions, if any, in cancer.

Despite the extensive literature describing associations between cathepsin H levels and patient prognosis, there is limited functional insight into the processes that this enzyme may regulate. Biochemical experiments have identified several extracellular proteins as cathepsin H substrates and those results have led some groups to speculate that this protease may enhance tumor invasion and metastasis (Tsushima et al., 1991). Another study has showed that this protease is involved in programmed cell death by cleaving the pro-apoptotic protein Bid following selective lysosomal disruption (Cirman et al., 2004). However, whether cathepsin H affects invasion, apoptosis or other tumorigenic processes *in vivo* is still an open question. Thus, we set out to gain further insight into the roles of cathepsin H in cancer through a genetic approach, by crossing *cathepsin H* null mice into the RIP1-Tag2 (RT2) model of tumorigenesis. RT2 mice develop multiple pancreatic islet tumors by 12-14 weeks of age as a consequence of expressing the SV40 T antigen in the insulin producing β cells (Hanahan, 1985). There are several reasons why we chose to use this particular model for the current study. First, it was previously found that cathepsin H expression is increased during RT2 tumorigenesis (Joyce et al., 2004), suggesting it may be involved in tumor progression or maintenance. Second, tumors in this model develop progressively through a series of discrete stages including hyperplastic islets, angiogenic islets and tumors. Thus by crossing *cathepsin H* deficient mice to RT2 animals, one can dissect the contribution of cathepsin H at each stage in the multistep tumorigenic pathway. We found that *cathepsin H* deficient RT2 mice had a reduction in angiogenic switching, developed fewer tumors and had an overall reduction in tumor volume. The resulting lesions had higher apoptosis rates, a reduction in proliferating cells and were less vascularized. Therefore, we conclude that

cathepsin H is involved in the establishment and maintenance of the tumor vasculature and is important for tumor formation and growth.

Results

In order to examine the role of cathepsin H in tumor development, we analyzed tumor progression in the RT2 model in the absence of this protease. *Cathepsin H* knockout mice have recently been generated and are viable and fertile with no gross phenotypes (Reinheckel and colleagues, manuscript in preparation). We generated *cathepsin H* null (*Ctsh*$^{-/-}$) RT2 mice and first analyzed the frequency of angiogenic switching at 10.5 weeks of age, which is a measure of the ability of pre-neoplastic lesions to induce neo-angiogenesis in their quiescent vasculature. In fact, this is a rate-limiting step in the RT2 model and determines the ability of subsequent tumors to develop. Cathepsin H is expressed at this stage of tumor progression, as determined by immunofluorescence staining of pancreatic tissue from 10.5 week old wild-type (WT) RT2 mice (data not shown). The angiogenic islets that formed, identified grossly by their red, hemorrhagic appearance, were counted in *Ctsh*$^{-/-}$ RT2 mice and the number was compared to the heterozygous or WT RT2 littermates. In the WT RT2 group, the number of islets ranged from 33 to 69, with an average of 52; in contrast, deletion of one or both copies of *cathepsin H* reduced the angiogenic switching frequency by 35% and 32%, respectively (Figure 1A; $P<0.01$).

Progression though angiogenic switching is essential for subsequent tumor development since an adequate blood supply is necessary for the expansive tumor growth that follows. Given the observed defect in angiogenic switching in RT2 mice lacking one or both copies of *Ctsh*, we next analyzed tumor development in these mice. We aged a separate cohort of mice to the defined endpoint of 13.5 weeks and assessed the tumor burden and incidence. Tumors, defined as lesions with a minimal diameter of 1 mm, were macroscopically detected and counted. In WT RT2 animals, the number of tumors ranged from 3 to 20, with a mean of 11.24. In contrast the mean tumor number in *Ctsh*$^{+/-}$ RT2 mice was reduced by 29% ($P<0.01$) and a further reduction to 33% ($P<0.01$) was observed upon deletion of the second copy of *Ctsh* (Figure 1B). These results closely parallel the percent reduction in the number of angiogenic islets, suggesting that the inability of one third of all islets to undergo angiogenic switching led to a comparable decrease in subsequent tumor incidence. When cumulative tumor volume was assessed in these same animals, a significant reduction of 40% was observed in *Ctsh* null RT2 mice (Figure 1C; $P<0.01$). In contrast, tumor volume in *Ctsh*$^{+/-}$ RT2 mice was only slightly impaired, despite the substantial decrease in the number of tumors, suggesting that the resulting lesions are not as significantly impaired in growth as lesions in *Ctsh* null animals. As tumors in *Ctsh*$^{+/-}$ RT2 mice were similar in size to the WT littermate controls, their phenotypes were not investigated further.

We hypothesized that the decrease in tumor volume in the *Ctsh* deficient RT2 mice is due to a shift in the balance between proliferation and apoptosis rates, which collectively affect tumor growth. First, we analyzed the proliferation rates by quantifying the number of BrdU-positive cells and determined that while there was a trend towards a reduction in *Ctsh* deficient tumors compared to WT RT2 tumors (30% decrease), this was not statistically significant (Figure 2A, B). To assess the effect of *cathepsin H* deletion on apoptosis we analyzed the number of cleaved caspase 3-positive cells in tumors from *Ctsh*$^{-/-}$ RT2 mice and compared them to WT RT2 littermates. The apoptotic index was increased two-fold ($P<0.05$) in the homozygous knockouts (Figure 2C, D), which together with the trend towards reduced proliferation, likely accounts for the significant reduction in tumor growth.

In addition to its role in apoptosis (Cirman et al., 2004), several studies have suggested that cathepsin H is involved in invasion, with numerous clinical reports documenting increased

cathepsin H expression in highly aggressive carcinomas (Berdowska, 2004). Therefore, we sought to assess the role of cathepsin H in invasion *in vivo* in the pancreatic islet cancer model. Pancreatic tissues from 13.5 week old RT2 mice were analyzed by hematoxylin and eosin (H&E) staining and the tumors were classified into three grades of increasing malignancy as previously described (Lopez and Hanahan, 2002). Briefly, encapsulated tumors are relatively benign lesions with an intact collagen capsule and a clear separation between the tumor and the surrounding normal exocrine pancreas. On the contrary, invasive carcinomas have migrated into the surrounding normal tissue. In the case of microinvasive carcinomas (IC1) there are focal regions of invasion with adjacent margins, while frankly invasive tumors (IC2) have widespread invasion with no evidence of tumor margins and are also characterized by an increased nuclear to cytoplasmic ratio (Lopez and Hanahan, 2002). Histological analysis of the spectrum of tumors revealed that while there was a slight decrease in the invasiveness of *Ctsh*$^{-/-}$ tumors, with less microinvasive and more benign lesions, there was no difference in the number of highly invasive carcinomas that developed (Figure 2E). Deletion of one allele of *cathepsin H* revealed an intermediate phenotype, which was also not statistically significant.

We next wanted to investigate whether cathepsin H plays a role in tumor angiogenesis as one explanation for the observed decrease in tumor growth in the *Ctsh* null RT2 mice is that there is an insufficient or poorly developed blood vasculature in the lesions. Moreover, we observed defects in angiogenic switching in *Ctsh*$^{-/-}$ RT2 animals (Figure 1A), suggesting that cathepsin H might have pro-angiogenic functions. Pancreatic tissue from 13.5 week old WT or *Ctsh* null RT2 mice was stained with an antibody recognizing the endothelial specific marker CD31 and several different parameters of the tumor vasculature were analyzed.

A reduction in vessels was observed in *Ctsh*$^{-/-}$ RT2 tumors, with a 32% decrease in area covered by CD31-positive structures relative to the control group (Figure 3A, B; $P<0.01$). To further characterize the angiogenic defects in *Ctsh*$^{-/-}$RT2 tumors, we perfused mice with a FITC-conjugated lectin, which binds to the luminal surface of endothelial cells thus labeling the vessels that are connected to the circulation. Measurement of the area of lectin covering the tumor vasculature showed that there was a 59% decrease in lectin perfusion in the *Ctsh*$^{-/-}$ RT2 tumors compared to WT, a reduction that was greater than the overall decrease in CD31 positive area (Figure 3A, C; $P<0.05$). Together these data suggested that some of the vessels that were present in *Ctsh*$^{-/-}$ RT2 tumors are not connected to the circulation and are therefore non-functional. To determine if this was indeed the case, we analyzed the co-localization of the lectin signal with that for CD31. We found that there was a reduction in the percentage of functional vessels in *Ctsh* deficient tumors and there was a corresponding increase in the number of CD31-positive vessels not filled with lectin compared to WT RT2 tumors.

One factor that can affect vessel integrity is their ability to recruit pericytes, which are a key component of the vasculature and can regulate vessel stability, maturation and function. While in normal vessels pericytes are in tight association with endothelial cells, in tumors pericytes are less abundant and more loosely attached to endothelial cells, with cytoplasmic processes that can extend away from the vasculature (Baluk et al., 2005). Co-staining of CD31 with the pericyte marker NG2 revealed a reduction in pericyte coverage of the blood vessels, calculated by the area of overlap between CD31 and NG2-positive areas, in *Ctsh* null tumors compared to WT RT2 controls (Figure 3D, E; $P<0.01$). Analysis of the ratio of NG2-positive area normalized to the vessel area revealed that there is no difference between WT and *Ctsh*$^{-/-}$ tumors in their ability to recruit pericytes in the vicinity of CD31-positive cells (Figure 3F). Rather the reduction in coverage was due to a defect in subsequent pericyte integration (calculated by the ratio of CD31+NG2+ area relative to CD31-NG2+) into the blood vessels in tumors lacking *Ctsh* (Figure 3G; $P<0.01$).

Given the angiogenic defects in the *Ctsh*$^{-/-}$ tumors at both the pre-neoplastic as well as tumor stage, we next wanted to determine the cellular source of this protease as expression by endothelial cells would suggest a cell-intrinsic effect for cathepsin H. However, immunofluorescence staining of WT RT2 tumors with cell type-specific antibodies revealed that cathepsin H is not expressed by CD31-positive endothelial cells, although many of the cathepsin H-positive cells are localized in close proximity to the vasculature (Figure 4A). Given the close interactions between endothelial cells and pericytes and the ability of mural cells to affect vessel integrity, we then investigated cathepsin H expression by pericytes by co-staining tissues with NG2; however, again no co-localization was observed (Figure 4B). Since certain inflammatory cells can also modulate tumor angiogenesis, we next stained RT2 tumors with antibodies against antigens present on neutrophils and macrophages. While there was no co-localization between cathepsin H protein and the neutrophil-specific antibody 7/4 (Figure 4C), this analysis revealed that the majority of cathepsin H expression is macrophage derived (Figure 4D). Cathepsin H expression by macrophages was verified using a second marker for this cell type, Iba1, and co-staining with CD31 showed that cathepsin H is often expressed by the macrophages in close proximity to the blood vessels (Figure 4E).

Discussion

In this study, we identify several tumor-promoting functions for cathepsin H in a mouse model of pancreatic islet cancer. *Cathepsin H* deficiency led to a significant reduction in tumor incidence and tumor growth. The resulting tumors were characterized by significantly increased apoptosis in association with a pronounced defect in tumor angiogenesis. Cathepsin H was also found to play important roles in angiogenic switching as well regulating certain characteristics of the tumor vasculature including vessel area, functionality and pericyte coverage.

Cathepsin H levels are upregulated in RT2 tumors (Joyce et al., 2004), however, the mechanisms leading to this upregulation are still unclear. We recently found that tumor secreted IL-4 induces cathepsin activity in tumor-associated macrophages (Gocheva et al., 2010). Therefore, IL-4 is a strong candidate for inducing cathepsin H upregulation, though likely not the only one as other factors have also been shown to mediate this effect. For example, interferon gamma and factor VIIa can both cause an increase in cathepsin H mRNA expression specifically in macrophages (Lafuse et al., 1995; Muth et al., 2005). Interestingly, in this study we found that cathepsin H is expressed at highest levels by the tumor-associated macrophages. This is also the case for several other members of the family, including cathepsin B and S (Gocheva et al., 2010; Vasiljeva et al., 2006), which are similarly upregulated during RT2 progression (Joyce et al., 2004). Importantly, macrophage-derived cathepsin activity for certain family members is critical in promoting tumor growth and angiogenesis in RT2 tumors (Gocheva et al., 2010). Additionally, macrophage-derived cathepsin B has been implicated in the development of lung metastasis in another cancer type using the MMTV-PyMT mouse model of breast cancer (Vasiljeva et al., 2006). Cathepsin H expression by macrophages has been observed in biopsies from patients with other cancer types as well giving a broader relevance to these results. For example, in melanoma, cathepsin H was detected mostly in infiltrating immune cells and in particular in macrophages adjacent to the tumor vasculature (Fröhlich et al., 2001). We observed a similar pattern in the RT2 tumors, with many of the cathepsin H-positive macrophages localizing close to the blood vessels. Interestingly, deletion of cathepsin H resulted in a significant reduction in vessel area, suggesting that cathepsin H supplied by the tumor infiltrating macrophages may be important for the formation and/ or maintenance of the vasculature.

These findings raise the question of how cathepsin H promotes tumor vascularization. One possibility is that cathepsin H can directly participate in remodeling of the extracellular matrix (ECM) and basement membrane (BM), which is a necessary step in the formation of new vessels. The BM and ECM are locally degraded to allow for the migration of endothelial cells toward angiogenic stimuli and to facilitate vessel sprouting, and it is possible that cathepsin H is one of the proteases that participates in this process. A few studies have demonstrated that cathepsin H can cleave certain ECM components, such as fibronectin (Tsushima et al., 1991), as well as degrade glomerular basement membrane (Davies et al., 1980; Thomas and Davies, 1989), thus lending support to this hypothesis. Typically, this degradation occurs extracellularly and in fact cathepsin H has been shown to be secreted from macrophages (Kominami et al., 1988) which would allow access to the extracellular environment. Moreover, several clinical reports have detected cathepsin H at substantial levels in the serum of cancer patients supporting the idea that it can be secreted during tumor progression (Berdowska, 2004).

Degradation of the vascular BM/ ECM can have a two-pronged effect on angiogenesis; it not only creates space for the developing vessels, but can also result in the release of active biomolecules that are sequestered in the matrix. In fact, several pro-angiogenic factors are bound to different ECM components and matrix degradation can lead to their release and activation. For example, FGF, a potent inducer of angiogenesis, is known to interact with heparan sulfate chains present in the ECM (Vlodavsky et al., 1996) and this interaction can modulate the activity of the downstream signaling pathway. Cathepsin H has been shown to hydrolyze the protein core of heparan sulfate proteoglycans (Thomas and Davies, 1989), which could potentially lead to FGF release and increased blood vessel formation. Whether this is the specific mechanism of action that explains the significant reduction in angiogenesis in *Ctsh*$^{-/-}$RT2 tumors warrants further investigation.

Cleavage of ECM components can result in increased bioavailability not just of pro-angiogenic growth factors, but also the release of chemokines that can stimulate vessel formation and enhance tumor progression (Wolf et al., 2008). Proteolytic processing of chemokines has recently emerged as an important mechanism for regulating their functions. Several years ago, Hasan and colleagues demonstrated that several chemokines from both the CXC and CC families are cathepsin B substrates (Hasan et al., 2006), which was one of the few studies to date to implicate cathepsins in the cleavage of these potent signaling molecules. The proteolytic activity of cathepsin B was restricted to the C-terminus of the identified substrates in this case; however, N-terminal processing of chemokines is a very important regulatory step that can amplify their biological activity (Wolf et al., 2008). Given that cathepsin H is an aminopeptidase and considering its potent effects on tumor progression and angiogenesis, it is possible that this protease also participates in chemokine processing, which could explain in part the phenotypes we have identified in *Ctsh*$^{-/-}$ RT2 mice.

Growth factors and chemokines enhance the proliferation of endothelial cells and thus stimulate angiogenesis; however, the tumor vascular network can also be expanded by the direct incorporation of endothelial progenitor cells (EPCs) into sprouting vessels (Gao et al., 2009). Whether EPCs contribute to a significant degree in angiogenesis in the RT2 model is still an open question, however, it is worth noting that two independent studies have reported the expression of cathepsin H in EPCs (Gao et al., 2008; Urbich et al., 2005). In a mouse model of lung metastasis it was determined that cathepsin H expression is increased three fold in tumor-recruited EPCs compared to those harvested from the bone marrow (Gao et al., 2008). Whether EPC-derived cathepsin H plays a role in tumor angiogenesis in this case or in RT2 tumors warrants further investigation.

Given these potential roles for cathepsin H in facilitating vascular BM/ ECM turnover during angiogenesis, it was somewhat surprising that we did not observe any significant effects on tumor invasion in *Ctsh*$^{-/-}$ RT2 mice, as several papers have speculated that cathepsin H plays a role in invasion due to its ability to cleave ECM components (Tsushima et al., 1991). Moreover, using cell culture assays, a decrease in glioblastoma cell invasion through Matrigel transwell assays was observed in the presence of a cathepsin H neutralizing antibody (Sivaparvathi et al., 1996). These results were most likely not due to direct matrix degradation by cathepsin H, as biochemical experiments have shown that this enzyme is unable to degrade collagen type IV or laminin (Tsushima et al., 1991), which are the two principal components in Matrigel (Kleinman and Martin, 2005). It is possible that cathepsin H can degrade other structural components in Matrigel and thus stimulate invasion in these specific examples. Similarly, differences in the BM/ ECM composition surrounding blood vessels compared to the tumor invasive front may dictate the relative abundance of cathepsin H substrates, and thus explain why cathepsin H affects one process and not the other.

In summary, we have identified roles for cathepsin H in promoting tumor development in a mouse model of cancer. Deletion of this protease resulted in poorly vascularized tumors, with additional angiogenic defects suggesting that cathepsin H plays important roles in the establishment and development of a functional tumor vasculature. The next step will be to search for specific substrates that can explain the underlying molecular mechanisms for the observed phenotypes. However, with this first genetic analysis of cathepsin H in an endogenous mouse model of cancer, we can now add cathepsin H to the growing list of proteases implicated in cancer development and progression.

Materials and methods

Transgenic mice

The generation and characterization of RIP1-Tag2 mice has been previously reported (Hanahan, 1985). Constitutive *Ctsh* null mice were generated by gene targeting in HM1-mouse embryonic stem cells (Reinheckel and colleagues, manuscript in preparation). Subsequently, *Ctsh* heterozygous mice were backcrossed into the C57BL/6 background for 9 generations before crossing to RT2 mice. All animal studies were performed using protocols approved by the animal care committee at Memorial Sloan-Kettering Cancer Center.

Tissue processing and analysis

RT2 mice were sacrificed by heart perfusion with PBS followed by 10% zinc-buffered formalin. Tumor-containing pancreas and control tissues were removed, placed in 30% sucrose overnight and embedded in OCT (Tissue-Tek, Torrance, CA). The dimensions of the tumors were measured with a ruler and their volume was calculated using the formula volume = width^2 × length × 0.52 to approximate the volume of a spheroid. Tumor burden was represented as the sum of the volumes of all tumors per mouse. Frozen sections (10 μm thick) were cut on a cryostat. For invasion grading, hematoxylin and eosin (H&E) staining was performed and the lesions were graded as previously described (Lopez and Hanahan, 2002), following a double-blind protocol and independently assessed by two investigators (VG and JAJ). For proliferation analysis, mice were injected i.p. with 100 ug/mg of bromodeoxyuridine (BrdU from Sigma, St. Louis MO) two hours prior to sacrifice. For the perfusion studies, mice were injected intravenously with a FITC-conjugated *Lycopersicon esculentum* lectin (100 μg in 100 μl, Vector Laboratories, Burlingame CA) 10 minutes prior to sacrifice. The numbers of tumors and mice analyzed are specified in the figure legends.

Immunohistochemistry

For immunofluorescence, the frozen sections were dried, preincubated with 1 × PNB blocking buffer and incubated with the primary antibody of interest overnight at 4°C. The following antibodies were used: rat anti-mouse CD31 (1:100; BD Pharmingen, San Diego CA), rabbit anti-mouse NG2 (1:200; Chemicon/ Millipore, Temecula CA), rat anti-mouse CD68 (1:1000; Serotec, Raleigh NC), rabbit anti-mouse Iba1 (1:1000; WAKO Chemicals USA, Richmond VA), rat anti-mouse 7/4 (1:200; Serotec), goat anti-mouse cathepsin H (1:1000; R&D Systems, Minneapolis MN), rabbit anti-mouse cleaved caspase 3 (1:500; Cell Signaling Technology, Beverly MA), rat anti-mouse BrdU (1:500; Serotec). The corresponding Alexa dye-tagged secondary antibodies (Invitrogen, Eugene OR) were used at a 1:500 dilution and incubated for 1h at room temperature. Species-matched immunoglobulins were used as negative controls. DAPI (1:2500, Invitrogen) was used to label the nuclei and the slides were mounted in ProLong Gold Mounting Medium (Invitrogen). The tissue sections were visualized under a Carl Zeiss Axioimager Z1 microscope and images were acquired with Axiovision using an Apotome (Zeiss) or with TissueFAXS (TissueGnostics, Vienna, Austria). For the apoptosis and proliferation analysis, the quantitation was performed using TissueQuest software (TissueGnostics) to determine the percentage of cleaved caspase 3-positive or BrdU-positive cells per tumor. For these analyses as well as the vasculature quantitation, individual fields of view were stitched using TissueFAXS to cover the entire tumor area. Vessel area and length were measured using Metamorph (Molecular Devices) and calculations were performed using established protocols (Xian et al., 2006). Briefly, pericyte coverage was measured by calculating the overlap of CD31 and NG2 signal in Metamorph. Pericyte recruitment was determined by dividing the NG2 stained area by the total CD31 area. Pericyte integration was calculated by the ratio of CD31+NG2+ area to the CD31-NG2+ area.

Statistical analysis

Data are expressed throughout as mean and SEM. Data were analyzed by unpaired Student's t-test and were considered statistically significant if $P < 0.05$. A cumulative logit model (McCullagh, 1980) with generalized estimating equations to correct for correlations within individual mice was used to compare the distribution of tumor grades for the control versus *CtsH* deficient RT2 mice.

Acknowledgments

We thank Kenishana Simpson for excellent technical assistance; Tanaya Shree for insightful comments on the manuscript; Stephanie Pyonteck and Karen Hunter for stimulating discussions. We are grateful to Elyn Riedel, MSKCC Epidemiology and Biostatistics Department, for statistical analysis and the MSKCC Molecular Cytology core facility for assistance with the Metamoph image analysis. This research was supported by the following: National Cancer Institute (NIH R01-CA125162) and the Geoffrey Beene Foundation (JAJ); Frank L. Horsfall Fellowship and Geoffrey Beene Fellowship (VG); the Deutsche Forschungsgemeinschaft SFB 850 Project B7 (TR, CP).

References

Baluk P, Hashizume H, McDonald DM. Cellular abnormalities of blood vessels as targets in cancer. Curr Opin Genet Dev. 2005; 15:102–111. [PubMed: 15661540]

Berdowska I. Cysteine proteases as disease markers. Clin Chim Acta. 2004; 342:41–69. [PubMed: 15026265]

Brix K, Dunkhorst A, Mayer K, Jordans S. Cysteine cathepsins: cellular roadmap to different functions. Biochimie. 2008; 90:194–207. [PubMed: 17825974]

Budihna M, Strojan P, Smid L, Skrk J, Vrhovec I, Zupevc A, Rudolf Z, Zargi M, Krasovec M, Svetic B, Kopitar-Jerala N, Kos J. Prognostic value of cathepsins B, H, L, D and their endogenous

inhibitors stefins A and B in head and neck carcinoma. Biol Chem Hoppe Seyler. 1996; 377:385–390. [PubMed: 8839984]

Cirman T, Oresic K, Mazovec GD, Turk V, Reed JC, Myers RM, Salvesen GS, Turk B. Selective disruption of lysosomes in HeLa cells triggers apoptosis mediated by cleavage of Bid by multiple papain-like lysosomal cathepsins. J Biol Chem. 2004; 279:3578–3587. [PubMed: 14581476]

Davies M, Hughes KT, Thomas GJ. Evidence that kidney lysosomal proteinases degrade the collagen of glomerular basement membrane. Ren Physiol. 1980; 3:116–119. [PubMed: 7034089]

del Re EC, Shuja S, Cai J, Murnane MJ. Alterations in cathepsin H activity and protein patterns in human colorectal carcinomas. Br J Cancer. 2000; 82:1317–1326. [PubMed: 10755408]

Fröhlich E, Schlagenhauff B, Möhrle M, Weber E, Klessen C, Rassner G. Activity, expression, and transcription rate of the cathepsins B, D, H, and L in cutaneous malignant melanoma. Cancer. 2001; 91:972–982. [PubMed: 11251949]

Gabrijelcic D, Svetic B, Spaić D, Skrk J, Budihna M, Dolenc I, Popovic T, Cotic V, Turk V. Cathepsins B, H and L in human breast carcinoma. Eur J Clin Chem Clin Biochem. 1992; 30:69–74. [PubMed: 1316176]

Gao D, Nolan D, McDonnell K, Vahdat L, Benezra R, Altorki N, Mittal V. Bone marrow-derived endothelial progenitor cells contribute to the angiogenic switch in tumor growth and metastatic progression. Biochim Biophys Acta. 2009; 1796:33–40. [PubMed: 19460418]

Gao D, Nolan DJ, Mellick AS, Bambino K, McDonnell K, Mittal V. Endothelial progenitor cells control the angiogenic switch in mouse lung metastasis. Science. 2008; 319:195–198. [PubMed: 18187653]

Gocheva V, Wang HW, Gadea BB, Shree T, Hunter KE, Garfall AL, Berman T, Joyce JA. IL-4 induces cathepsin protease activity in tumor-associated macrophages to promote cancer growth and invasion. Genes Dev. 24:241–255. [PubMed: 20080943]

Gocheva V, Wang HW, Gadea BB, Shree T, Hunter KE, Garfall AL, Berman T, Joyce JA. IL-4 induces cathepsin protease activity in tumor-associated macrophages to promote cancer growth and invasion. Genes Dev. 2010; 24:241–255. [PubMed: 20080943]

Hanahan D. Heritable formation of pancreatic beta-cell tumours in transgenic mice expressing recombinant insulin/simian virus 40 oncogenes. Nature. 1985; 315:115–122. [PubMed: 2986015]

Hasan L, Mazzucchelli L, Liebi M, Lis M, Hunger RE, Tester A, Overall CM, Wolf M. Function of liver activation-regulated chemokine/CC chemokine ligand 20 is differently affected by cathepsin B and cathepsin D processing. J Immunol. 2006; 176:6512–6522. [PubMed: 16709808]

Joyce JA, Baruch A, Chehade K, Meyer-Morse N, Giraudo E, Tsai FY, Greenbaum DC, Hager JH, Bogyo M, Hanahan D. Cathepsin cysteine proteases are effectors of invasive growth and angiogenesis during multistage tumorigenesis. Cancer Cell. 2004; 5:443–453. [PubMed: 15144952]

Kageshita T, Yoshii A, Kimura T, Maruo K, Ono T, Himeno M, Nishimura Y. Biochemical and immunohistochemical analysis of cathepsins B, H, L and D in human melanocytic tumours. Arch Dermatol Res. 1995; 287:266–272. [PubMed: 7598531]

Kleinman HK, Martin GR. Matrigel: basement membrane matrix with biological activity. Semin Cancer Biol. 2005; 15:378–386. [PubMed: 15975825]

Kominami E, Tsukahara T, Hara K, Katunuma N. Biosyntheses and processing of lysosomal cysteine proteinases in rat macrophages. FEBS Lett. 1988; 231:225–228. [PubMed: 3360126]

Kos J, Smid A, Krasovec M, Svetic B, Lenarcic B, Vrhovec I, Skrk J, Turk V. Lysosomal proteases cathepsins D, B, H, L and their inhibitors stefins A and B in head and neck cancer. Biol Chem Hoppe-Seyler. 1995; 376:401–405. [PubMed: 7576236]

Lafuse WP, Brown D, Castle L, Zwilling BS. IFN-gamma increases cathepsin H mRNA levels in mouse macrophages. Journal of Leukocyte Biology. 1995; 57:663–669. [PubMed: 7722423]

Lecaille F, Kaleta J, Bromme D. Human and parasitic papain-like cysteine proteases: their role in physiology and pathology and recent developments in inhibitor design. Chem Rev. 2002; 102:4459–4488. [PubMed: 12475197]

Lopez T, Hanahan D. Elevated levels of IGF-1 receptor convey invasive and metastatic capability in a mouse model of pancreatic islet tumorigenesis. Cancer Cell. 2002; 1:339–353. [PubMed: 12086849]

McCullagh P. Regression models for ordinal data. J Royal Stat Soc. 1980; 42:109–142.

Muth H, Kreis I, Zimmermann R, Tillmanns H, Holschermann H. Differential gene expression in activated monocyte-derived macrophages following binding of factor VIIa to tissue factor. Thromb Haemost. 2005; 94:1028–1034. [PubMed: 16363246]

Reinheckel, T.; Gocheva, V.; Peters, C.; Joyce, JA. Roles of Cysteine Proteases in Tumor Progression. In: Edwards, D.; Hoyer-Hansen, G.; Blasi, F.; Sloane, BF., editors. The Cancer Degradome. Springer; New York: 2008. p. 281-304.

Sivaparvathi M, Sawaya R, Gokaslan ZL, Chintala SK, Rao JS, Chintala KS. Expression and the role of cathepsin H in human glioma progression and invasion. Cancer Letters. 1996; 104:121–126. [PubMed: 8640738]

Thomas GJ, Davies M. The potential role of human kidney cortex cysteine proteinases in glomerular basement membrane degradation. Biochim Biophys Acta. 1989; 990:246–253. [PubMed: 2923904]

Tsushima H, Ueki A, Matsuoka Y, Mihara H, Hopsu-Havu VK. Characterization of a cathepsin-H-like enzyme from a human melanoma cell line. Int J Cancer. 1991; 48:726–732. [PubMed: 2071233]

Urbich C, Heeschen C, Aicher A, Sasaki K, Bruhl T, Farhadi MR, Vajkoczy P, Hofmann WK, Peters C, Pennacchio LA, Abolmaali ND, Chavakis E, Reinheckel T, Zeiher AM, Dimmeler S. Cathepsin L is required for endothelial progenitor cell-induced neovascularization. Nat Med. 2005; 11:206–213. [PubMed: 15665831]

Vasiljeva O, Dolinar M, Turk V, Turk B. Recombinant human cathepsin H lacking the mini chain is an endopeptidase. Biochemistry. 2003; 42:13522–13528. [PubMed: 14621998]

Vasiljeva O, Papazoglou A, Kruger A, Brodoefel H, Korovin M, Deussing J, Augustin N, Nielsen BS, Almholt K, Bogyo M, Peters C, Reinheckel T. Tumor cell-derived and macrophage-derived cathepsin B promotes progression and lung metastasis of mammary cancer. Cancer Res. 2006; 66:5242–5250. [PubMed: 16707449]

Vasiljeva O, Reinheckel T, Peters C, Turk D, Turk V, Turk B. Emerging roles of cysteine cathepsins in disease and their potential as drug targets. Curr Pharm Des. 2007; 13:387–403. [PubMed: 17311556]

Vlodavsky I, Miao HQ, Medalion B, Danagher P, Ron D. Involvement of heparan sulfate and related molecules in sequestration and growth promoting activity of fibroblast growth factor. Cancer Metastasis Rev. 1996; 15:177–186. [PubMed: 8842489]

Waghray A, Keppler D, Sloane BF, Schuger L, Chen YQ. Analysis of a truncated form of cathepsin H in human prostate tumor cells. J Biol Chem. 2002; 277:11533–11538. [PubMed: 11796715]

Wolf M, Albrecht S, Marki C. Proteolytic processing of chemokines: implications in physiological and pathological conditions. Int J Biochem Cell Biol. 2008; 40:1185–1198. [PubMed: 18243768]

Xian X, Hakansson J, Stahlberg A, Lindblom P, Betsholtz C, Gerhardt H, Semb H. Pericytes limit tumor cell metastasis. J Clin Invest. 2006; 116:642–651. [PubMed: 16470244]

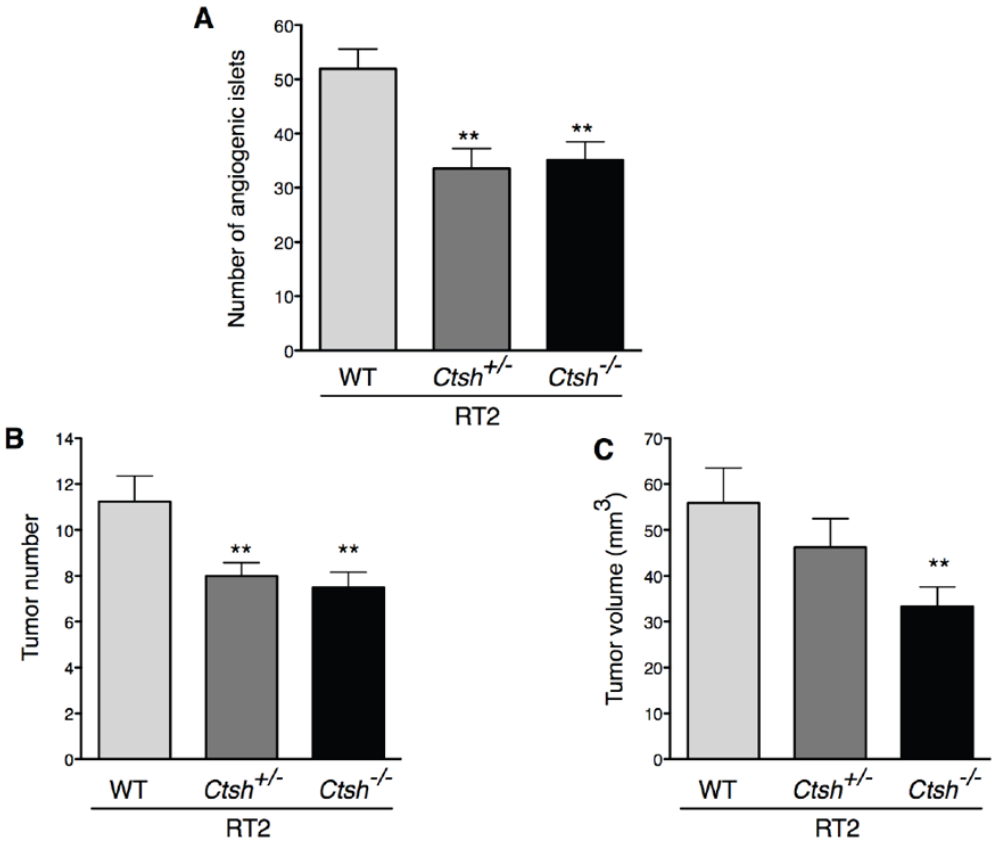

Figure 1. Deletion of *cathepsin H (Ctsh)* in RT2 mice leads to a reduction in angiogenic switching, tumor number and tumor volume

(A) The number of angiogenic islets was assessed at 10.5 weeks in WT, $Ctsh^{+/-}$ and $Ctsh^{-/-}$ RT2 littermates. The graph represents the average number of angiogenic islets per mouse. The following numbers were analyzed: WT RT2: 10 mice; $Ctsh^{+/-}$RT2: 15 mice; $Ctsh^{-/-}$ RT2: 12 mice. ** P<0.01 compared to WT.

(B) The number of tumors was counted in WT, $Ctsh^{+/-}$ and $Ctsh^{-/-}$ RT2 littermates at 13.5 weeks of age. The graph represents the average number of tumors per mouse. The following numbers were analyzed: WT RT2: 21 mice; $Ctsh^{+/-}$ RT2: 56 mice; $Ctsh^{-/-}$ RT2: 32 mice. ** P<0.01 compared to WT.

(C) Cumulative tumor volume, represented as the sum of the volumes of all tumors per mouse, was calculated in 13.5 week old WT, $Ctsh^{+/-}$ and $Ctsh^{-/-}$ RT2 littermates and revealed a significant reduction in tumor growth upon complete deletion of *Ctsh*. The following numbers were analyzed: WT RT2: 21 mice; $Ctsh^{+/-}$ RT2: 56 mice; $Ctsh^{-/-}$ RT2: 32 mice. ** P<0.01 compared to WT.

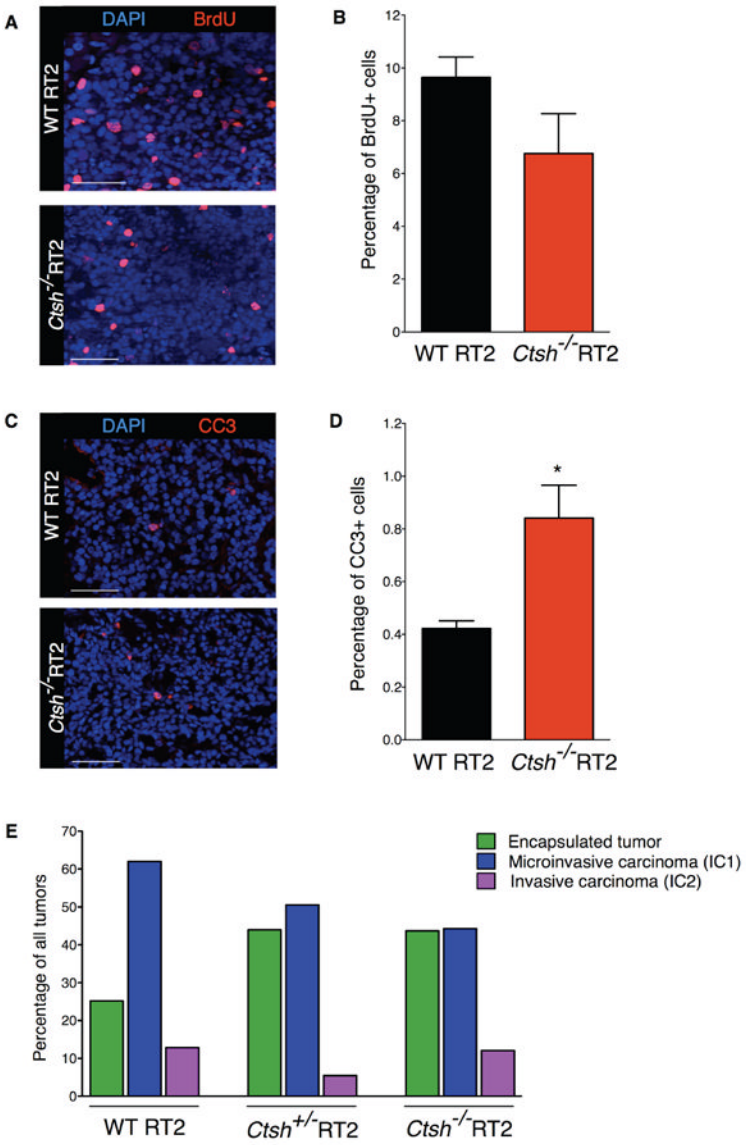

Figure 2. C*athepsin H* deletion affects the balance between apoptosis and proliferation in RT2 tumors

(A) Representative images of proliferating cells in WT and *Ctsh* null RT2 tumors as detected by BrdU incorporation. Scale bars 50 μm.

(B) The percentage of BrdU-positive cells per tumor was determined with TissueQuest analysis software. Graph showing the average percentage of tumor proliferation per mouse in each group. n=6 mice in each group.

(C) Representative images of cleaved caspase 3 (CC3) stained tumors from 13.5 week old WT and *Ctsh*$^{-/-}$ RT2 mice showing a greater abundance of apoptotic cells in the *Ctsh* null group. Scale bars 50 μm.

(D) The percentage of apoptotic (CC3-positive) cells was quantified per tumor using TissueQuest analysis software. Graph showing the average percentage of tumor apoptosis per mouse in each group. * P<0.05 compared to WT; n=5 mice in each group.

(E) Deletion of cathepsin H has no significant effect on tumor invasion. Graph showing the proportion of encapsulated tumors, microinvasive (IC1) and invasive carcinomas (IC2) in 13.5 week old WT RT2, *Ctsh*$^{+/-}$ RT2 and *Ctsh*$^{-/-}$ RT2 littermates. Tumors were graded from

H&E stained sections independently and in a blinded fashion by two investigators. The following numbers were analyzed: WT RT2: 12 mice; *Ctsh*$^{+/-}$ RT2: 11 mice; *Ctsh*$^{-/-}$ RT2: 11 mice.

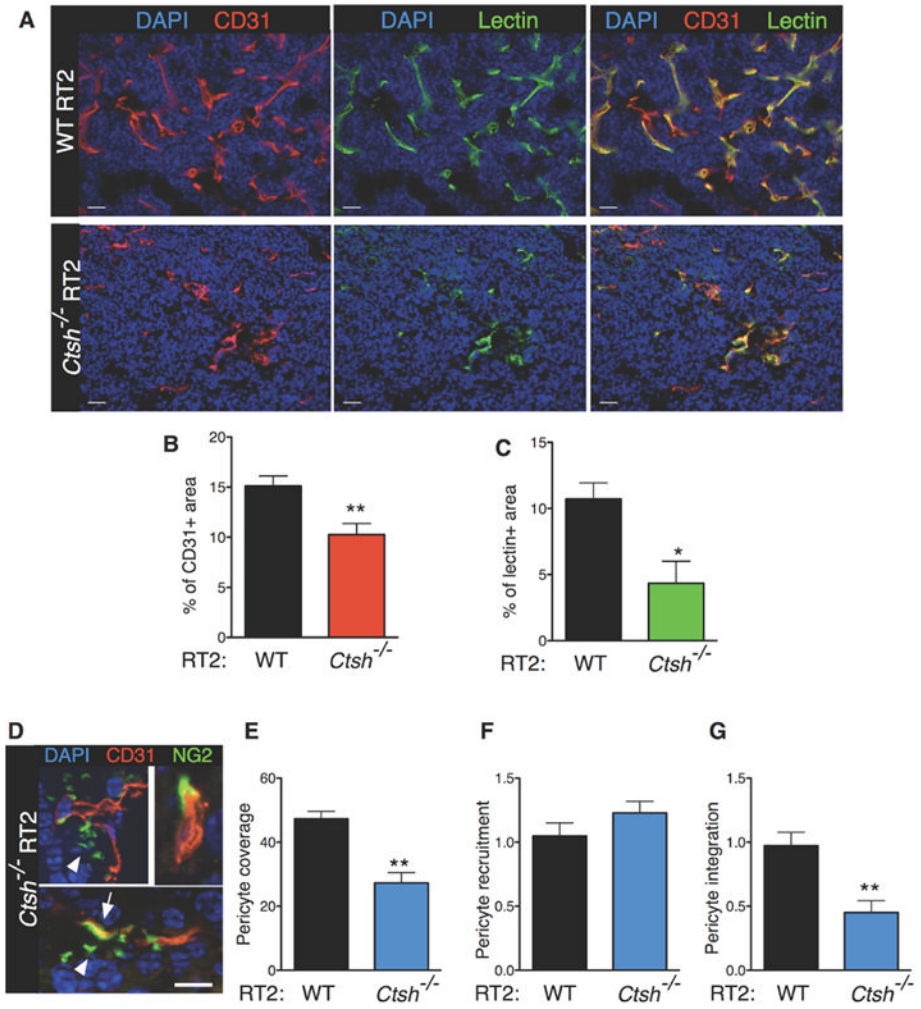

Figure 3. Cathepsin H has important roles in regulating tumor angiogenesis

(A) Representative images of the vasculature of 13.5 week old WT and *Ctsh*$^{-/-}$ RT2 tumors. Scale bars 50 μm.

(B) The vessel area was calculated as the ratio of CD31-positive endothelial cells divided by the DAPI-positive tumor area as detected by pixel intensity and analyzed using Metamorph imaging software. ** P<0.01 compared to WT; n=15 mice for WT RT2 group; n=12 for the *Ctsh*$^{-/-}$ RT2 group.

(C) The area of functional vessels was analyzed by calculating the area of lectin signal divided by the DAPI-positive tumor area. * P<0.05 compared to WT; n=5 mice in each group.

(D) A collage of three high power representative images of the pericyte coverage in *Ctsh*$^{-/-}$ RT2 tumors. We observed that often the NG2-positive pericytes were not closely associated with CD31-positive endothelial cells (arrowhead) although complete co-localization of the two markers (arrow) was also evident in other vessels. All images were taken at the same magnification and the scale bar length is 50 μm.

(E) Pericyte coverage was measured by calculating the overlap of CD31 and NG2 signal in WT and *Ctsh*$^{-/-}$ RT2 tumors using Metamorph imaging software. n=5 mice for WT RT2 group; n=4 for the *Ctsh*$^{-/-}$ RT2 group.

(F) Pericyte recruitment was determined by dividing the NG2 stained area by the total CD31-positive area. n=5 mice for WT RT2 group; n=4 for the *Ctsh*$^{-/-}$RT2 group.

(G) Pericyte integration was calculated by the ratio of CD31+NG2+ area to the CD31-NG2+ area. n=5 mice for WT RT2 group; n=4 for the *Ctsh*$^{-/-}$RT2 group.

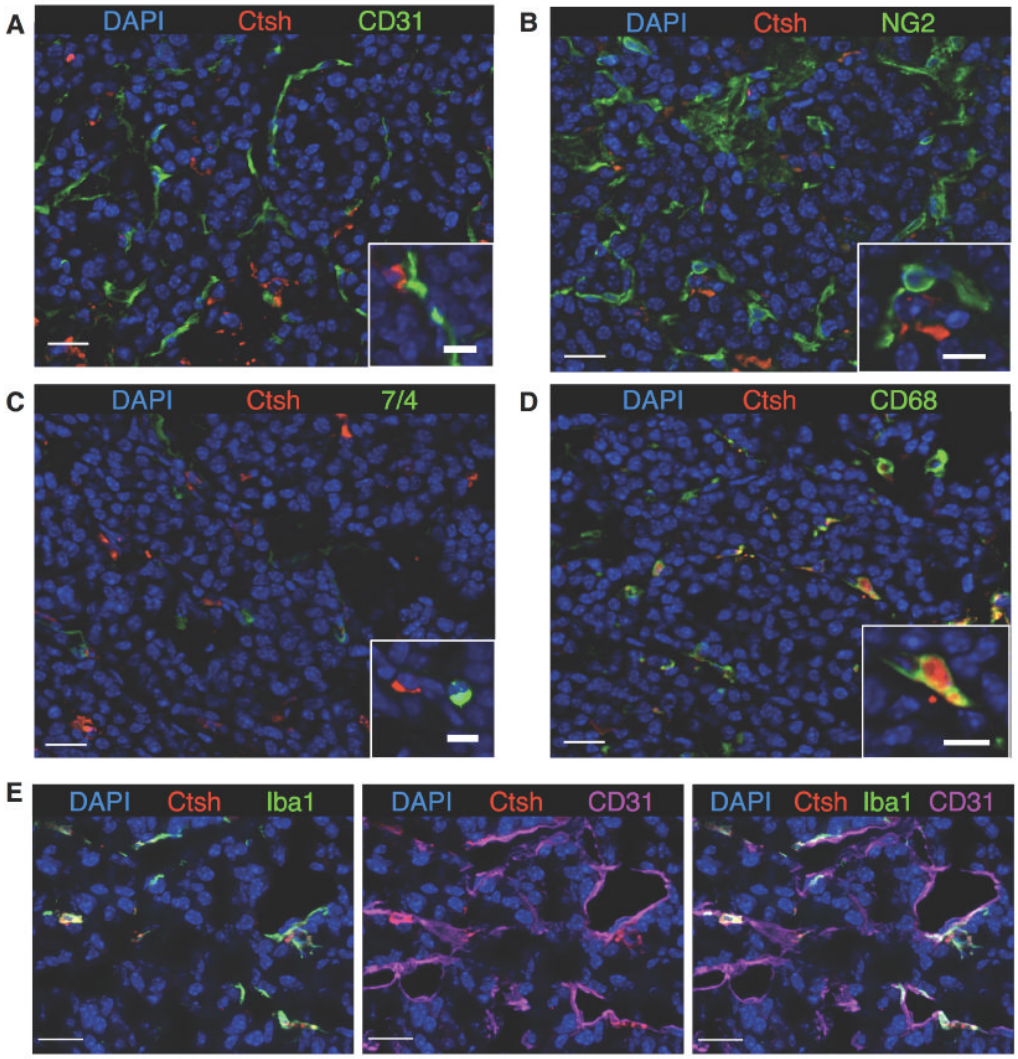

Figure 4. Analysis of cathepsin H expression in WT RT2 tumors

Immunostaining with a number of cell type-specific antibodies revealed that cathepsin H is not expressed by CD31-positive endothelial cells (A), NG2-positive pericytes (B) or 7/4-positive neutrophils (C), but the main source of cathepsin H are the CD68-positive tumor-associated macrophages (D).

(A-D) Scale bars for large panels are 20 μm. Scale bars in the inserts are 10 μm.

(E) Cathepsin H localizes to perivascular macrophages as identified by their expression of Iba1 and localization close to the CD31-positive vessels. Scale bars 20 μm.